SAND2006-6622P

ANALYSIS OF DIRECT BRINE RELEASE FOR PERFORMANCE ASSESSMENT OF THE WASTE ISOLATION PILOT PLANT

Teklu Hadgu, Byoung Yoon Park and Palmer Vaughn

Sandia National Laboratories

ABSTRACT

This paper documents the development, implementation, and results of an analysis of direct brine release (DBR) at the Waste Isolation Pilot Plant (WIPP), for the technical baseline migration (TBM). Direct brine releases are the releases to the surface of dissolved radionuclides in the brine phase during the drilling of exploratory boreholes that penetrate the repository at some future time. The TBM represents incremental enhancements to the performance assessment (PA) baseline that was used to support the certification of the WIPP. These improvements include improved representation of the conceptual understanding of the physical and chemical processes (i.e., natural and engineered barrier systems) that control releases to the environment. One of the more important changes is the explicit inclusion of the Option D panel closure.

The direct brine release simulations for the TBM applied the BRAGFLO_DBR baseline model with some incremental changes. The TBM DBR calculations included three scenarios that were selected to represent the undisturbed case (S1) and two disturbed cases, S3 and S5. For each scenario, DBR calculations were performed for two well locations (down dip and up dip) at specified intrusion times.

Results show that S1 and S5 result in decreased DBR compared to the original baseline. The main reason for the low brine releases for S1 and S5 is the implementation of Option D panel closure. S3 has more significant brine releases than S1 and S3, and generally slightly higher releases than the original baseline. The S3 releases from the TBM implementation are also directly attributed to the effectiveness of the Option D panel closure system in isolating the intruded panel from the rest of the repository.

1. INTRODUCTION

The direct brine release (DBR) model simulates the flow of brine and gas to the surface as a result of inadvertent drilling into a pressurized repository at some future time. The repository waste contains, in part, steel, cellulosics, plastics, and rubbers which can produce gases when exposed to brine. This gas generation may result in increased pressures over time. Therefore, a future driller that unknowingly penetrates through the site may experience a forced flow of brine and gas. DBR is modeled as two-phase flow of brine and gas from the repository to the surface through the annulus of the drill string and the open hole. This involves transient porous medium flow in the repository coupled to steady vertical flow in the borehole. Porous medium flow in the repository is simulated using the numerical code BRAGFLO, and the Poettmann-Carpenter correlation (Poettmann and Carpenter, 1952) is used to simulate two-phase vertical flow in a borehole. The wellbore flow model is coupled to the BRAGFLO code through a wellbore boundary condition that is used to represent flow in the wellbore. An iterative procedure was used to obtain a "look-up" table in the form of a curve fit to produce flowing bottomhole pressure (the boundary condition) as a function of flow variables (brine pressure and saturation). Further details can be found in Helton et al. (1998).

1.1 Background

The Waste Isolation Pilot Plant (WIPP) is a deep geologic repository for the disposal of transuranic (TRU) waste generated by national defense activities. The WIPP site is located in Eddy County in southeastern New Mexico about 26 miles southeast of the City of Carlsbad. The WIPP underground disposal area is mined at a depth of about 658.5 m (2,160 feet) beneath the surface in ancient salt beds of the Salado Formation (Figure 1). The WIPP facility has been designed to dispose of up to 168,500 cubic meters of contact-handled and 7,080 cubic meters of remote-handled TRU waste.

In 1996 the Department of Energy (DOE) submitted the compliance certification application (CCA) for the operation of the WIPP (DOE, 1996). In May 1998, the Environmental Protection Agency (EPA) certified that the WIPP would comply with the radioactive waste disposal regulations of 40 CFR Part 191. The first shipment of TRU waste arrived at the WIPP for disposal in March 1999.

A focus of the simulations that were used as part of WIPP certification was a Performance Assessment (PA), which evaluated the potential for radioactive materials to migrate to the accessible environment over a 10,000-year period. The PA was based on a compendium of conceptual models for features, events, and processes that could affect repository performance, software applications that implement the conceptual models, and parameter values and their associated distributions that form inputs to the software applications.

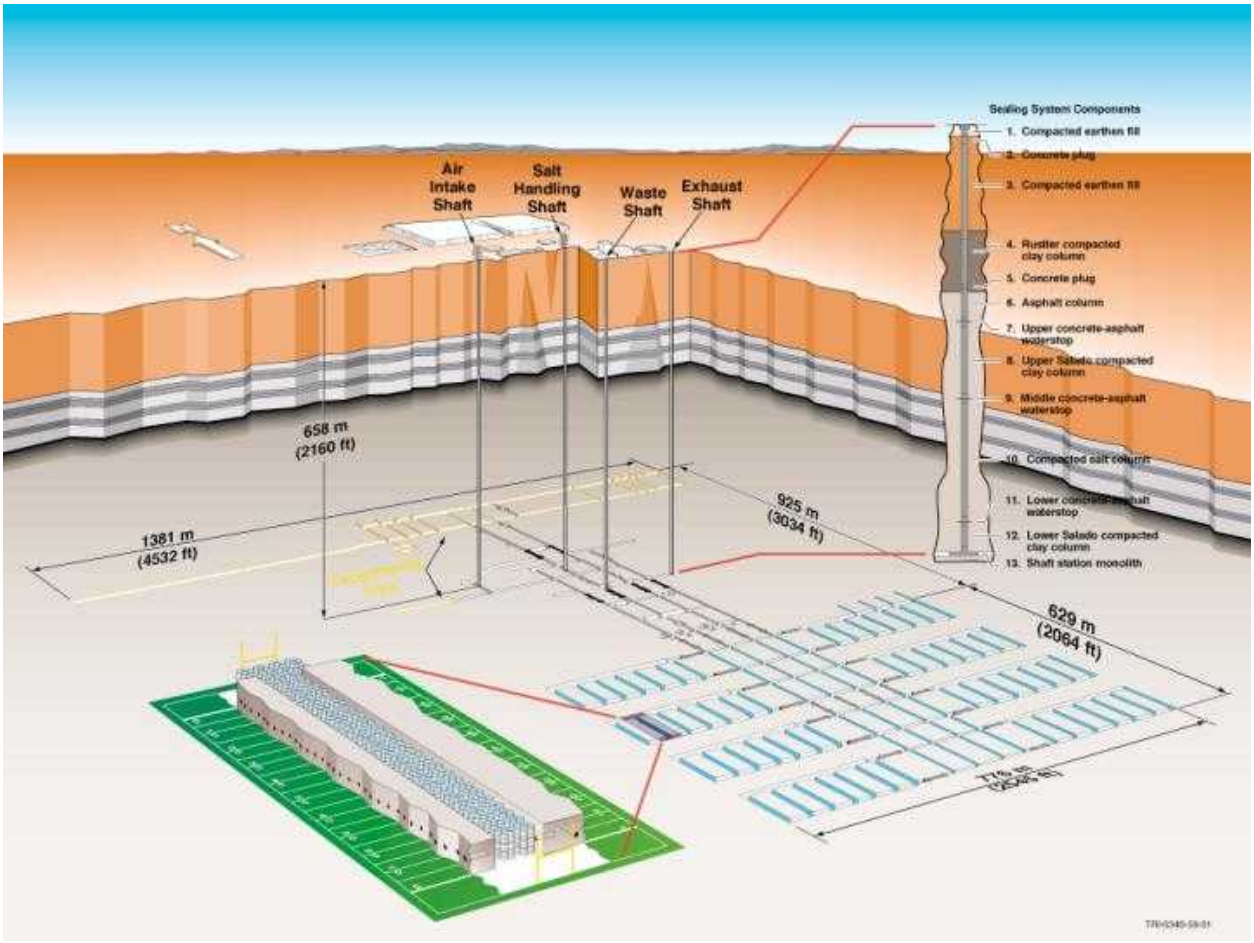

Figure 1: The WIPP Repository Layout

1.2 Conditions for Direct Brine Release

Certain conditions must exist within the waste disposal areas in order for brine to flow directly to the surface during a drilling intrusion:

- Pressure in the waste disposal areas of the repository must be greater than that exerted by a column of drilling fluid that penetrates a waste panel (8 MPa). This is the minimum pressure needed to overcome the hydrostatic head of the drilling fluid.

- There must be mobile brine present in the waste panels for contaminated brine to flow through the consolidated waste to the borehole and upward to the surface. Iron corrosion consumes brine and releases gas as a by-product, and it is possible for the brine volume in the waste pores to drop below its residual saturation because of this process.

1.3 Overview of the CCA/PAVT DBR Model

The 10,000-year BRAGFLO regional model used in the CCA and the Performance Assessment Verification Test (PAVT) calculations represents the WIPP repository and formations around the WIPP site using a two-dimensional, quasi-radial, geometric approach. The waste disposal areas of the repository are represented by a single panel in one region and the rest of the waste disposal panels in another region called the rest of the repository (ROR). Three-dimensional details are incorporated using a radial-flaring approach to simulate three-dimensional geometry with a two dimensional grid. The grid used for DBR modeling is a "repository scale" model which includes greater detail of the waste panel geometry. This detail was deemed necessary to better capture the short term and near field response to a borehole intrusion into the repository. The grid was set up as a two-dimensional finite difference mesh of 39 × 39 grid blocks to be solved using BRAGFLO (hereafter the direct brine release version will be called BRAGFLO_DBR). The mesh compares to the 10,000-year model (hereafter called BRAGFLO) in the following ways:

- The BRAGFLO_DBR mesh is oriented in the areal plane that includes the repository, with the z-dimension (height) one element thick and reflecting the collapsed height of the repository at the time of borehole penetration. The BRAGFLO mesh is oriented as a vertical cross-section, with multiple layers in height, and the thickness (z-dimension) one element thick. The thicknesses of the grid blocks preserve repository dimensions and account for far field radial flow patterns.

- BRAGFLO_DBR models flow only through the waste disposal areas of the repository. The BRAGFLO model includes the surrounding geology as well as the entire WIPP excavation (including operations and experimental regions).

- Local scale heterogeneities are included in the BRAGFLO_DBR model, including the salt pillars, waste rooms, panel seals, and passageways, which contain waste. These are not fully represented in the BRAGFLO mesh.

- The BRAGFLO_DBR mesh uses constant thickness, while BRAGFLO radially flares the element thickness to account for three-dimensional volumes in two-dimensional space.

- The disturbed rock zone (DRZ) is included in both models, but exists above and below the excavated regions in the BRAGFLO model, whereas the DRZ surrounds the waste rooms on the sides for the BRAGFLO_DBR model. Composite effective properties are also used to include the effect of the DRZ above and below the repository in BRAGFLO_DBR. The DRZ is a region of rock adjacent to the excavated areas containing micro fractures caused by the excavating process and therefore has enhanced permeability compared to the undisturbed rock.

- Both models include one-degree formation dip through the excavated regions.

Helton et al. (1998, Sections 4.7 and 10) and McKinnon and Freeze (1997) provide more details on the BRAGFLO_DBR model used in the CCA and PAVT.

The DBR analysis uses the following two-phase equations to calculate flow from the repository into a well at constant flowing-bottomhole pressure:

$$q_p = J_p(P_p - P_{wf}) \quad (1)$$

Where, P_p = repository pressure, P_{wf} = flowing bottomhole pressure

q_p = phase volume flow rate (brine or gas)

J_p = phase productivity index (brine or gas)

The phase productivity index is defined as:

$$J_p = \frac{2\pi k k_{rp} h}{\mu_p \left[\ln\left(\frac{r_e}{r_w}\right) + s + c \right]} \quad (2)$$

Where, k = intrinsic permeability, k_{rp} = phase residual saturation

r_e = equivalent radius of grid block containing intrusion borehole

r_w = well radius, h = crushed panel height

μ_p = phase viscosity, s = skin factor

c = -0.50 for pseudo steady-state

A response surface was used to provide flowing bottom-hole pressure values as a function of repository pressure and saturation at the time of intrusion and other repository properties. The response surface was generated using an iterative procedure based upon a multiphase wellbore flow correlation developed by Poettmann and Carpenter (1952). The response surface was designed to represent expected ranges of panel pressures, brine saturation, critical gas saturation, panel permeability, crushed panel height and wellbore skin factor due to solid releases.

The Technical Baseline Migration (TBM) is a modeling analysis that follows the CCA/PAVT. The TBM represents incremental enhancements to the performance assessment (PA) baseline that was represented by the CCA/PAVT calculations. The direct brine release simulations for the TBM applied the BRAGFLO_DBR model that was used for the 1996 CCA and the 1997 PAVT calculations with some incremental changes discussed in Section 2 of this paper, and a correction discussed below.

A factor 2π was missing from the productivity index (PI) equation used in BRAGFLO_DBR calculations in the CCA and PAVT (shown in the denominator of Equation 1, above). Correcting the PI equation resulted in changes to the response surface for flowing bottom-hole pressure. As a result a new response surface was used for the TBM.

1.4 WIPP Performance Assessment Scenario Conceptualization

The PA process considers the natural and man-made processes and events that could affect the disposal system, as well as probable release mechanisms from the disposal system, and

formulates scenarios. Scenarios are representations of the evolution of the disposal system and are composed of specific combinations of features, events, and processes. Cumulative radionuclide releases from the disposal system are calculated for each scenario considered and probabilities of the scenarios are assigned for each realization of the modeling system to construct distributions of Complementary Cumulative Distribution Functions (CCDFs). The WIPP PA considered scenarios for undisturbed performance and disturbed performance. Thus, potential releases from both human-initiated activities (e.g., via drilling intrusions) and natural processes (e.g., via dissolution) that would occur independent of human activities were assessed. The results of the performance assessment simulations illustrate the potential releases of radioactive materials from the disposal system to the accessible environment over the 10,000-year regulatory period.

Conceptually, there are several pathways for radionuclide transport within the undisturbed disposal system that may result in releases to the accessible environment. Contaminated brine may migrate away from the waste-disposal panels if pressure within the panels is elevated by the generation of gas from corrosion or microbial degradation. Radionuclide transport may occur laterally, through the anhydrite marker beds toward the subsurface boundary of the accessible environment in the Salado, or through access drifts or anhydrite marker beds (primarily Marker Bed (MB) 139) to the base of the shafts. In the latter case, if the pressure gradient between the panels and overlying strata is sufficient, then contaminated brine may migrate up the shaft seals. As a result, radionuclides may be transported directly to the ground surface, or they may be transported laterally away from the shafts, through permeable strata such as the Culebra, toward the subsurface boundary of the accessible environment. These conceptual pathways are shown in Figure 2.

Disturbed performance is dominated by the deep drilling scenarios, which involve at least one deep drilling event that intersects the waste disposal region. If a borehole intersects the waste in the disposal rooms, releases to the accessible environment may occur as material entrained in the circulating drilling fluid is brought to the surface. Particulate waste brought to the surface may include cuttings, cavings, and spallings. Cuttings are the materials cut by the drill bit as it passes through the waste. Cavings are the materials that may be forced into circulating drilling fluid as a result of the shearing action of the drealing fluid on the waste. Cavings and cuttings realizes are assumed to be independent of the conditions that exist in the repository at the time of a drilling intrusion.. Spallings are the materials transported up the borehole by venting gas after a drilling intrusion. During drilling, contaminated brine may flow up the borehole and reach the surface, depending on fluid pressure within the waste panels. This direct flow of contaminated brine to the surface is what is accounted as direct brine release (DBR). The deep drilling event may also involve the penetration of a pocket of brine in the Castile formation below the waste panel thus providing a connection for brine flow from the Castile to the waste panel. The conceptual pathways for disturbed performance due to a deep drilling event are shown in Figure 3.

In the WIPP PA there are a total of six scenarios defined (S1 through S6). The Technical Baseline Migration (TBM) DBR calculations that are the subject of this study included three of these scenarios. The three scenarios were selected to represent the undisturbed case (S1) and two disturbed cases (S3 and S5, first intrusions at 1000 years into the repository and underlying brine pocket and repository only, respectively). Scenarios 2 and 4, with 350 year first intrusions result in lower releases due to the shorter time period for repository pressures to build up(Hansen et al.,

2002). To reduce computation effort, the TBM concentrated on the scenarios with potentially larger releases. For each scenario DBR calculations were performed for two well locations (down dip and up dip) at the specified intrusion times given below.

- **Scenario 1** – represents an undisturbed repository in the 10,000-year BRAGFLO runs. For direct brine release an S1 scenario examines the release of contaminated brine to the surface during the first intrusion into a previously undisturbed repository. First intrusions are simulated at Time = 100, 350, 1000, 3000 and 10,000 years.

- **Scenario 3** – represents an intruded repository at Time = 1000 years in the 10,000-year BRAGFLO runs. The intrusion penetrates the repository and a brine pocket below. For direct brine release an S3 scenario examines the release of contaminated brine to the surface during a second intrusion into the repository following a previous intrusion that penetrated the repository and an underlying brine pocket at 1000 years. Second intrusions are simulated at Time = 1200, 1400, 3000, 5000 and 10,000 years.

- **Scenario 5** – represents an intruded repository at Time = 1000 years in the 10,000-year BRAGFLO runs. The intrusion borehole penetrates the repository only and does not extend to the brine pocket. For direct brine release an S5 scenario examines the release of contaminated brine to the surface during a second intrusion into the repository following a previous intrusion that penetrated only the repository at 1000 years. Second intrusions are simulated at Time = 1200, 1400, 3000, 5000 and 10,000 years.

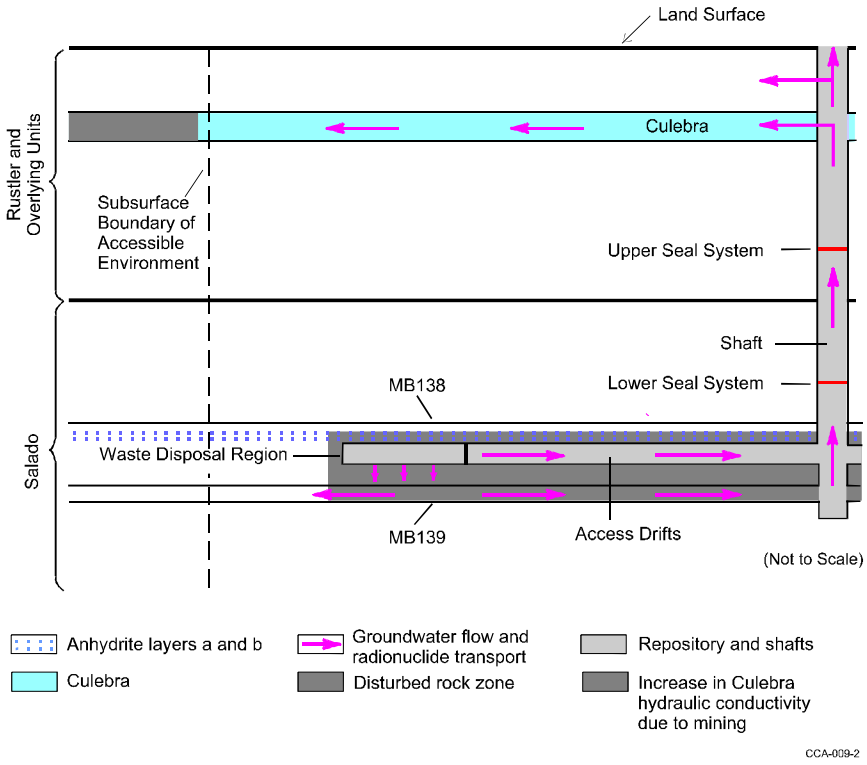

Figure 2: Conceptual Pathways for Undisturbed Performance

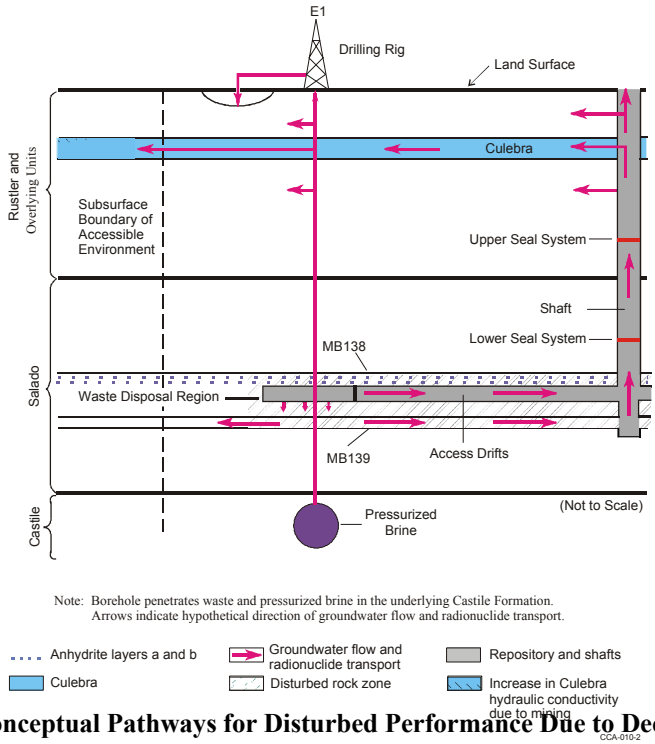

Figure 3: Conceptual Pathways for Disturbed Performance Due to Deep Drilling

2. CHANGES MADE FOR THE TECHNICAL BASELINE MIGRATION

Since the completion of the CCA and PAVT and EPA's certification of the WIPP repository, conceptual understanding of the physical and chemical processes that control releases to the environment has improved, the 2π error in the productivity index equation discussed in Section 1.3 been identified in the baseline calculation that requires correction, and a specific panel closure design (Option D) that was not modeled in the CCA has been specified by the EPA (US EPA, 1998). The focus of this paper is on these modeling changes, although Option D panel closure and other aspects of the calculations have been subsequently superseded. The following discussion addresses the changes in the BRAGFLO computational grid and the changes in the BRAGFLO material properties used for the TBM simulations. Since it is important that these changes are consistently applied through out the WIPP PA modeling system, corresponding changes are also required to appropriately model DBR using BRAGFLO_DBR.

2.1 BRAGFLO Computational Grid

The primary assumption affecting the formulation of the BRAGFLO computational grid is that spatial processes in the vicinity of the repository can be adequately represented in a two-dimensional domain. As such, the BRAGFLO simulations of long-term fluid flows in the Salado and overlying units are executed with a vertical two-dimensional grid that comprises a cross-section on a north-south axis (the X axis of the grid) directly through the repository. The vertical dimension of the repository corresponds to the Y-axis of the grid. Flows convergent to and divergent from the waste regions are accommodated in a grid-flaring scheme in which the depth

of grid elements perpendicular to the X-Y plane (the Z axis of the grid) are increased with horizontal distance from the waste regions.

2.1.1 Baseline Computational Grid

For the CCA and PAVT calculations, the computational grid for brine and gas flow used a single disposal-system geometry that had 1023 elements (a 33 × 31 element grid), together with dimensions of the elements. Horizontal grid spacing in the excavated region was controlled largely by the dimensions of repository features (e.g. the shaft and intrusion borehole). Horizontal spacing to the north and south of the excavated region started at 10 m and increased by a factor of 2-5 out to 20 km beyond the Land Withdrawal Boundary (LWB). Vertical spacing at the repository level was controlled by the dimensions of the excavated regions and marker beds. In the upper Salado, vertical spacing was controlled by the thickness of shaft seal materials. For units above the Salado, vertical spacing was controlled by the thickness of each major geologic formation.

Effects of flow in the third (out-of-plane) dimension were approximated with a two-dimensional element configuration that simulated convergent or divergent flow to the north and south, centered on the repository. Several scales of radial flaring were included (local-scale flaring around the intrusion borehole and shaft, and regional-scale flaring around a point near the north end of the rest of the repository). This simplifying assumption was compared three-dimensional model simulations and found to be acceptable because the computed releases to the accessible environment for both representations were nearly equivalent (Vaughn, 1996). This indicated that, based on the performance measures and the overall uncertainty, the two-dimensional model was sufficient for calculating releases.

2.1.2 TBM Computational Grid

The most important changes to the BRAGFLO computational grid include: (1) general refinements of the X- and Y-dimensions of grid cells, (2) modification of the flaring scheme for varying the Z-dimension of cells, (3) removal of the shaft seal system from the model domain, and (4) implementation of the Option D panel closures. The BRAGFLO TBM computational grid is shown in Figure 4. To identify the relative importance of these changes, an intermediate simulation study was conducted using items (1) and (2) above. The intermediate study (referred to as Technical Baseline Intermediate, TBI) included only changes identified in items (1) and (2), with everything else as in the PAVT. Results of the TBI along with the TBM and PAVT are discussed in Section 3.

Grid cell dimensions in the baseline grid increase in the north-south direction by a factor of about 5 with distance away from the repository. The TBM grid addresses this issue by using a refinement factor of 1.45 outside the repository. In addition the TBM grid fixes a vertical refinement problem near Marker Bed 139, where the grid aspect ratio between neighboring grids was high.. One effect of these changes will be to reduce numerical dispersion in the transport calculations

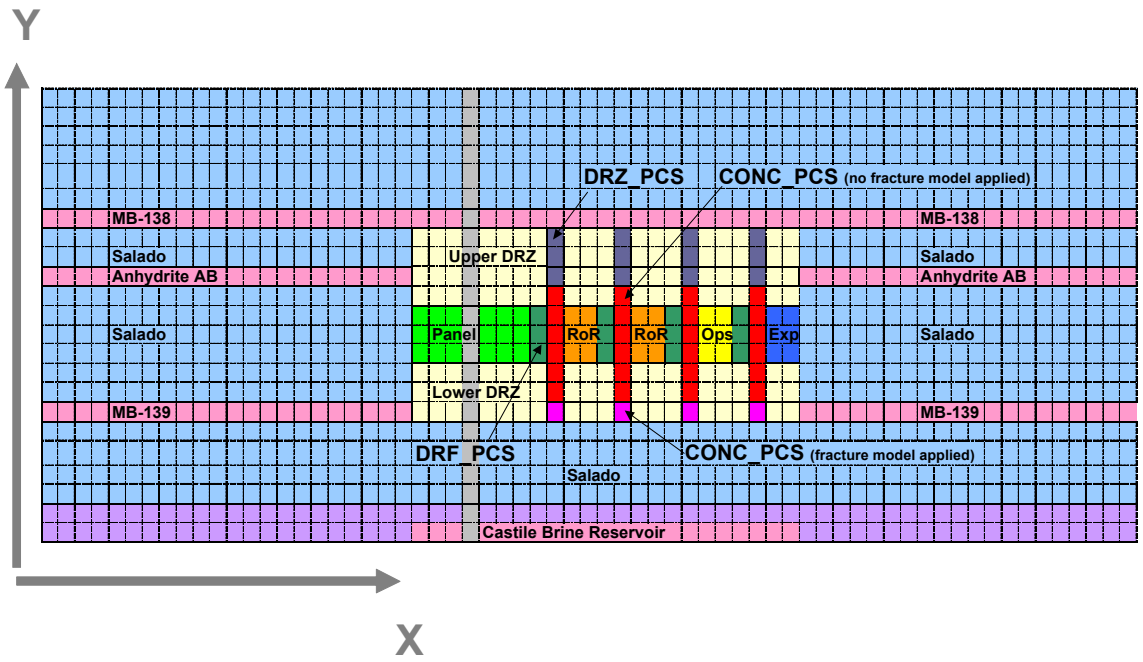

Figure 4: TBM BRAGFLO Grid

2.1.3 Implementation of Option D Panel Closures

Implementation of Option D (Figure 5) is designed to provide the least fluid flow between panels. The compliance baseline calculations from the CCA and PAVT do not explicitly model the Option D configuration, however. Changes in material properties of the panel closure and neighboring DRZ, as well as refinement of grid geometry were deemed necessary in order to capture the physical effects of the Option D closure system.

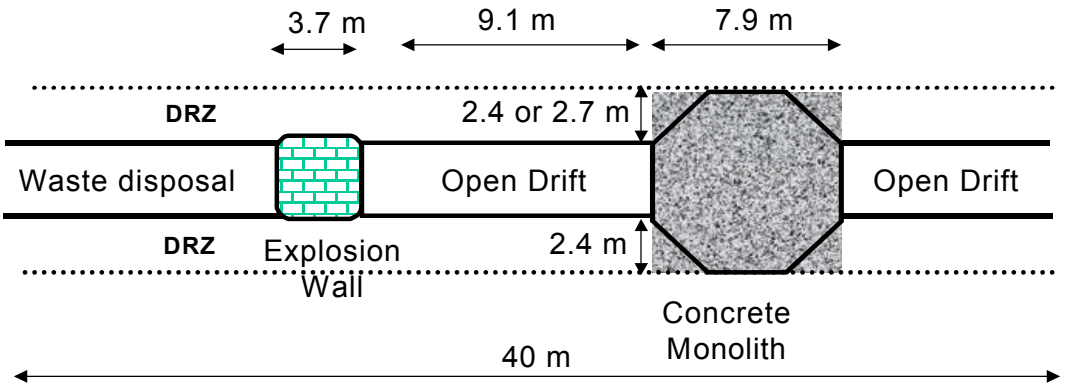

Figure 5: Side View of Option D Panel Closure

Figures 6 compares the panel closure implementation in the CCA/PAVT and TBM grids. There are several important differences. First, the TBM grid extends the concrete into the upper and lower DRZ, as called for in the Option D design (Figure 5). Furthermore, while the baseline

model approach lumped the panel closure into one column of three cells with uniform properties, the TBM divides the panel closure and surrounding materials into a system of four materials in 13 grid cells including:

1. Six cells of panel closure concrete represented by the material CONC_PCS.
2. Three cells of healed DRZ above the panel closure system (PCS) represented by the material DRZ_PCS.
3. Three cells of empty drift and explosion wall represented by the material DRF_PCS.
4. One cell of panel closure concrete that is embedded in MB 139 represented by the material CPCS_F.

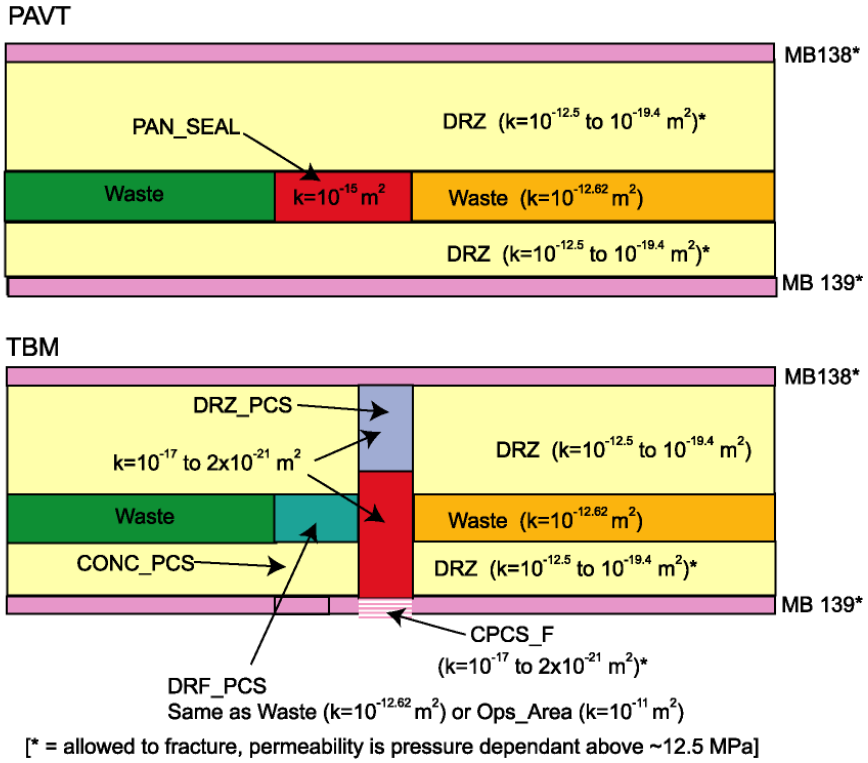

Figure 6: Panel Closures in PAVT and TBM

Unlike the baseline panel closure representation, which allowed significant and rapid brine and gas flow between different regions of the repository, the Option D panel closures are designed to impede such flows. For the TBM, four sets of panel closures were included in the model domain **(**Figure 4**).** These panel closures lie in between the following grid regions: the single intruded waste panel, southern rest of repository, northern rest of repository, operations area, and experimental area.

2.2 BRAGFLO Material Properties

In support of the TBM, several BRAGFLO materials and their property values have been added and/or updated. Those materials are shown in Figure 4 and include:

1. DRZ_1: material representing the DRZ above and below the repository excluding the DRZ above the PCS
2. DRZ_PCS: material representing the DRZ above the PCS
3. CONC_PCS: material representing panel closure concrete
4. DRF_PCS: material representing the empty drift and explosion wall
5. CPCS_F: material representing panel closure concrete that is embedded in MB 139

2.2.1 TBM Disturbed Rock Zone

In the TBM conceptualization of the DRZ, the permeability and porosity in the DRZ are represented as they were for the PAVT. However, because there is a 12 m section of Salado halite between the repository and MB 138 and halite is not very susceptible to fracturing, it has been decided that the anhydrite fracture model should not be applied to the DRZ above the repository.

Within the lower DRZ the fracture model has been retained from the PAVT. There is only a 2 m section of Salado halite between the repository floor and MB 139. As rooms close, the floor heaves and fractures, and in the presence of higher gas pressures, fractures are not expected to heal thereby, maintaining a hydraulic connection to MB 139. For this reason, the pressure dependent anhydrite fracture model is applied only to the DRZ *below* the repository in the current conceptualization of the DRZ.

2.2.2 Panel Closure Concrete

A specific panel closure system (Option D) has been added to the conceptualization of the WIPP repository and the PA integrated system model has been modified accordingly. Option D requires the use of a salt-saturated concrete, identified as Salado mass concrete, as designed for the shaft seal system. The design of the shaft seal system included various material properties that are described in Hurtado et al. (1997). The TBM BRAGFLO grid incorporates a new material, CONC_PCS, which is assigned the material properties of Salado mass concrete and is used to represent the concrete monolith of the Option D panel closure system.

One of the assumptions at the time of the CCA was that cementacious materials used in the shaft seal system would degrade after 400 years. This assumption was considered conservative and

gave greater confidence to the redundant, multi-barrier design of the shaft seal system. It is not at all clear that a similar assumption would be conservative for the Option D panel closures. Thompson and Hansen (1996) estimated that only minor degradation would be expected for the concrete members of the panel closure concrete during the regulatory period. They determined that potential flow through the concrete closure would be nearly two orders of magnitude too small to cause any significant degradation of the concrete component. Although the inclusion of the Option D panel closure requires a new material, CONC_PCS, the property values used at the time of certification for a related parameter used to represent undegraded Salado mass concrete are used for CONC_PCS.

2.2.3 Disturbed Rock Zone Above the Panel Closure

The design of Option D panel closures requires the removal of the DRZ above and below the panel entry drifts. The depth of cut below the floor will mine out MB 139. Loose salt in the roof also will be taken down just prior to construction of the concrete monolith. The remaining salt surrounding the panel closure concrete will be subjected to compressive stresses, which will facilitate the rapid healing of disturbed zones. Owing to the rounded configuration of Option D, the compressive stress state creates a situation very favorable for concrete: high compressive stresses and low stress differences. In turn, the compressive stresses developed within the salt will quickly heal any damage caused by construction excavation, thereby eliminating the DRZ along the length of the panel closure. The salt immediately above and below the rigid concrete monolith component of Option D will approach the intrinsic permeability of the Salado halite.

To capture the healed DRZ above the panel closure concrete monoliths requires a new material, DRZ_PCS, in the BRAGFLO grid. The property values assigned to DRZ_PCS are the same as those values used for a similar DRZ-related material (DRZ_1) at the time of certification, except for the properties PRMX_LOG, PRMY_LOG, and PRMZ_LOG, the logarithm of permeability in the X, Y, and Z directions, respectively. These permeability values are assigned the same distributions used for the new material CONC_PCS. In this instance, the values are based on the nature of the model set-up, and not directly on experimental data (although the general range of the distribution agrees with experimental observations of healed salt).

The use of these permeabilities ensures that fluid flow is equally probable through or around the Option D panel closures and best represents the uncertainty that exists in the performance of the panel closure system.

2.2.4 Empty Drift and Explosion Wall Materials

DRF_PCS is the material representing the empty drift and explosion wall. This material has properties equivalent to the material representing the waste panel (except it is not filled with waste) and is used for the three panel closures that are adjacent to waste regions. The creep closure model is applied to this material to be consistent with the neighboring materials. The non-concrete portion of the northernmost panel closure between the operations area and the experimental area is assigned properties equivalent to the operations area. This is done so that the creep closure model is applied consistently to different regions in the grid (the waste regions have the creep closure model applied whereas the operations area is modeled as pre-closed and assigned an initial low porosity for all times).

2.2.5 Panel Closure Concrete Embedded in MB 139

CPCS_F is the material representing the plug of panel closure concrete that is embedded in MB 139. At low pressures, CPCS_F has the same properties as CONC_PCS. At high pressures, CPCS_F is allowed to fracture similar to the anhydrite Marker Bed 139 located at the same level.

The application of the fracture model simulates a fluid pathway around the panel closure in the event that fracture pressures are reached. Such a pathway is reasonable because floor heave will cause fracturing of the lower DRZ, establishing a hydraulic path to Marker Bed 139. Flow around panel closures through MB 139 is a possibility if pressures exceed fracture initiation levels. In these cases, a two-dimensional grid doesn't allow such flows to be modeled directly. Instead the effect of such flow is simulated by allowing the lowermost cell of the concrete monolith to fracture as in MB 139. In this way significant flow around the panel closure is simulated only when pressures are quite high. The application of the fracture model to this material is reasonable since the concrete permeability range is very close to the range used for the anhydrite marker beds.

2.2.6 Molecular Weight of Cellulose

In order to calculate gas generation, the BRAGFLO code uses the molecular weight of the cellulosic material, which undergoes microbial degradation. However, the TRU waste inventory includes a variety of cellulosic materials, which are represented by a single material and molecular weight in BRAGFLO. The molecular weight of the form of cellulose thought to best represent the composite of cellulosic materials in the repository is with the molecular formula, $C_6H_{10}O_5$. Specifically, the carbon-normalized molecular weight of cellulose in TBM was lowered from 30.026×10^{-3} kg/mol for CH_2O to 27.023×10^{-3} kg/mol for $C_6H_{10}O_5$.

A reduction in the molecular weight corresponds to an increase in the total number of moles of carbon available for gas production, and thus, more total gas can be produced.

2.3 DBR Model Changes Leading to the TBM Implementation of BRAGFLO_DBR

The DBR model that was used in the CCA and PAVT calculations is used in this study with some changes. These changes were made partly to be consistent with the changes introduced to the 10,000-year BRAGFLO TBM calculations (discussed above in Sections 2.1 and 2.2), to improve on DRZ representation in the BRAGFLO_DBR implementation, and to correct any errors.

Changes were made to the DBR CCA/PAVT implementation in order to make a TBM version of BRAGFLO_DBR that is consistent with BRAGFLO TBM (Figure 4**).** The changes include correcting the missing 2π in the productivity equation, changing the molecular weight of cellulose, and the changes discussed in Sections 2.3.1, 2.3.2 and 2.3.3,

The three corresponding waste disposal regions in the BRAGFLO_DBR TBM numerical mesh are shown in Figure 7. The coupling between the TBM vertical and horizontal grids is shown in Figure 8.

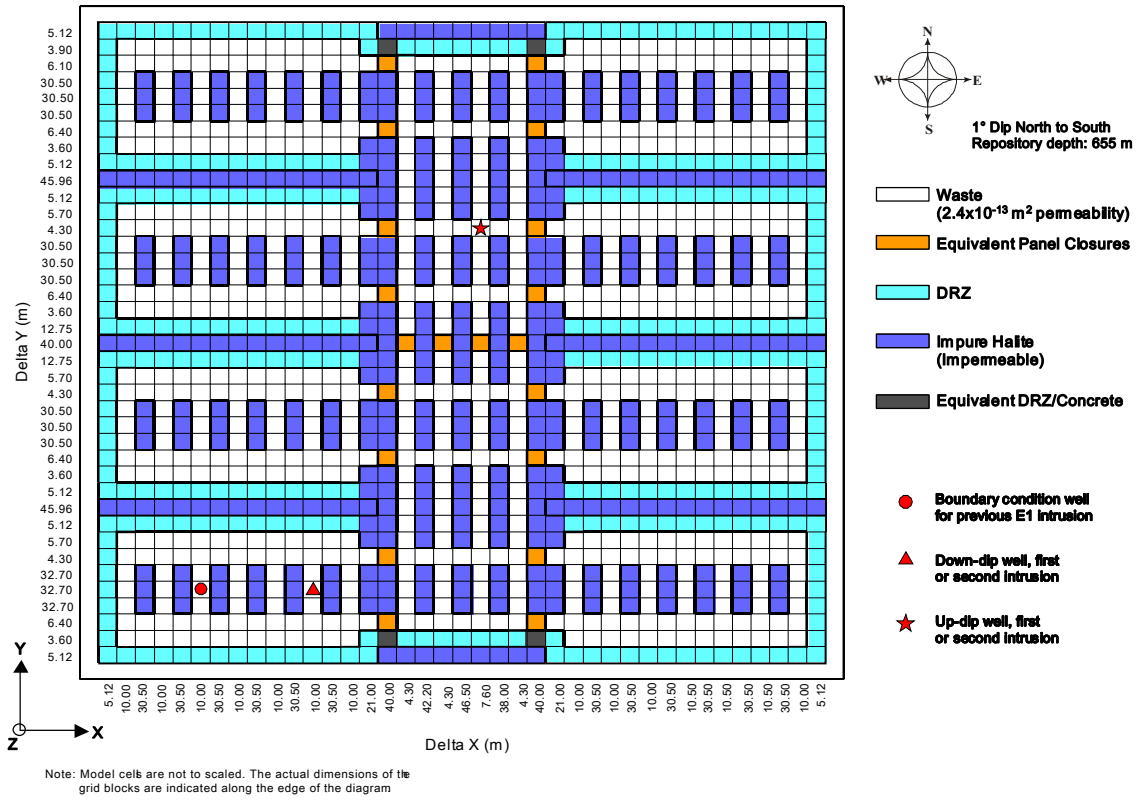

Note: Model cells are not to scaled. The actual dimensions of the grid blocks are indicated along the edge of the diagram

Figure 7: TBM horizontal grid (logical)

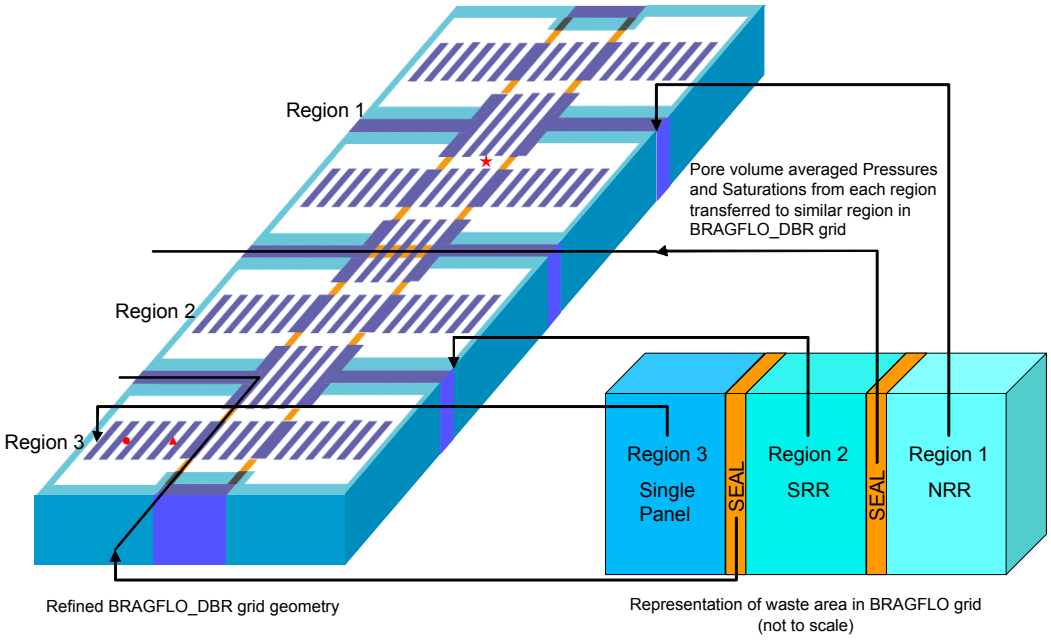

Figure 8: Representation of coupling of grids to provide initial conditions for DBR: TBM

2.3.1 Introducing Option D Panel Closure in DBR

To minimize changes to the BRAGFLO_DBR TBM grid and to ease the computational burden, the panel closure was represented with collective equivalent properties. Since the drift (DRF_PCS) contains most of the pore volume of the panel closure, the rest of the material properties for the equivalent system will be the same as DRF_PCS. In the 10,000-year BRAGFLO TBM calculations DRF_PCS was given properties of the waste area, including creep closure (for panel closures in the waste-area) but excluding waste inventory and gas generation. Thus, all properties for the panel closure, with the exception of permeability and porosity, will be the same as that of WAS_AREA.

For determining the collective equivalent properties of permeability and porosity, the concrete part of the Option D panel closure has been represented by CONC_PCS, ignoring the CPCS_F portion. This is because DBR is interested at the level of the repository, and also because of the assumption that the fracturing in CPCS_F will not have a significant effect on brine releases. The 10,000-year BRAGFLO TBM calculations showed that CPCS_F fracturing occurs in only a few vectors. In addition the BRAGFLO_DBR analysis includes fracturing in the lower DRZ. For permeability and porosity, effective values representing the concrete and the drift parts were used. The effective permeabilities and porosities are calculated as follows**.** The effective permeability in the x-direction (for two materials in series) is a harmonic average of the two permeabilities. The effective permeability (for two materials in parallel) is a length weighted average of the two permeabilities.

2.3.2 Changing CCA/PAVT Representation of DRZ in the DBR Grid

A study of the BRAGFLO_DBR results for the PAVT (MacKinnon and Freeze, 1997) shows that when DRZ permeabilities are high, the entire repository becomes hydraulically connected during a DBR calculation. Such cases could produce unrealistic brine releases when combined

with high pressures and high brine saturations and do not represent an improved understanding of the characteristics or extent of the DRZ, which indicates that the DRZ only extends a couple of meters into the walls of the rooms and is not expected to provide a ready conduit of fluids between separate panels and around panel closures. To implement the current understanding of the DRZ, it was necessary to change the material assignments made to the BRAGFLO_DBR grid for the TBM (see Figures 7 and 8). The following is a description of the DRZ related changes that were made:

- For the pillars between rooms (within a panel), physically the outer edges (a few meters deep) would be DRZ and the inner core would be Salado Halite. For brine release calculations these pillars could be represented by an effective permeability consisting of Salado Halite and DRZ. Because the size of the inner core is large compared to the DRZ outer edges, the effective permeability would be nearly the same as the Salado Halite. Thus, the effective permeability of the pillars is represented as Salado halite.

- The massive pillar between panel closures would also have DRZ in the outer edges. With an Option D panel closure any DRZ in contact with the panel closures will heal. As discussed above, the effective permeability for this case would be very close to that of the Salado halite. Thus, it was represented as Salado halite.

- In the CCA and PAVT the material between the full panels is represented as 5.12 m of DRZ, 45.96 m of Salado Halite and 5.12 m of DRZ. Whatever the permeability of the DRZ, the 45.96 m thick Salado Halite will prevent any flow between the full panels. However, flow could occur in the 5.12 m thick DRZ surrounding the full panels. Thus, the 5.12 m thick DRZ is assigned the DRZ permeability at the time of intrusion.

Near the outer edges of the DBR mesh, the 3.60 m and 3.90 m thick boundary DRZ next to panel closures will be affected by the presence of the Option D panel closure. The extension of the panel closure's concrete will penetrate through the DRZ thickness in either case (i.e. 3.6 m or 3.9 m). Thus, as was done with the vertical extension of the concrete into the DRZ in the TBM grid, a similar horizontal extension was introduced in the TBM DBR grid. The 40 m length DRZ grid blocks next to the panel closure (Delta X in Figure 7) has been divided into 7.9 m of concrete and 32.1 m of DRZ. The dimensions correspond to the drift and concrete part of the panel closure. Since the DRZ part has a much larger pore volume than the concrete part, a decision was made to use DRZ material properties, with the exception of permeability and porosity, to represent the equivalent material. As was done for the panel closures (Section 2.3.1), effective permeabilities and porosity were used to represent the permeabilities and porosity of the two materials. For the TBM calculations for DRZ, panel closure and halite relative permeability and capillary pressure input parameter values, which were specified in the 10,000-year BRAGFLO calculations were used to assure consistency.

2.3.3 Porosity in Non-Waste Regions (DRZ, halite and Panel Closure)

In the DBR model the vertical thickness of the DBR grid is assigned the compacted panel height calculated at the time of intrusion. Assigning the same thickness (the compacted panel height) to all grid blocks in the DBR grid means that the pore volumes of the non-repository materials (i.e. DRZ, halite and panel closure) in the 10,000-year vertical BRAGFLO grid are not properly

represented in the DBR grid. To account for this the porosities of these non-repository materials used in the DBR calculations are proportionally increased.

Based on the need to keep DRZ material pore volumes in the two grids equivalent, an initial height was calculated for the DRZ. For the TBM implementation the same DRZ initial height as in the CCA and PAVT was used.

2.4 BRAGFLO_DBR CALCULATION METHOD

Direct brine release simulations for the TBM adopted the calculation method used in both the CCA and the PAVT. Direct brine release calculations are carried out after the 10,000-year BRAGFLO calculations are completed. The pressure and saturation time-histories for each scenario from the 10,000-year BRAGFLO calculations provide the basic input needed for the direct brine releases. The pressure and saturation at specified times for each vector furnish the initial and boundary conditions needed for the BRAGFLO_DBR model to determine the volume of direct brine releases to the surface. The initial condition values are also used to determine the flowing bottomhole pressure in the intruding borehole (boundary condition for wellbore flow). The model assumes no-flow boundary conditions beyond the confines of the BRAGFLO_DBR numerical mesh (Figure 7**)** for the flow period (up to 11 days) of direct releases, i.e. there is no connection to the surrounding geology. All relevant flow parameters (permeability, porosity, characteristic curves, etc.), both sampled (stochastic) and unsampled (deterministic), are the same as those used for the 10,000-year BRAGFLO model.

3. ANALYSIS OF CALCULATION RESULTS

Following is an analysis of the calculation results for the TBM implementation of BRAGFLO_DBR, and comparisons with PAVT results. The impact of repository brine pressure and saturation on direct brine release is assessed by comparing the TBM BRAGFLO repository brine pressure and saturation histories against the minimum requirements needed to produce brine at the surface, i.e. repository pressure and brine saturation at the time of intrusion must exceed 8 MPa and residual brine saturation, respectively. The reported brine pressures and saturations are volume-averaged values, which are averaged over all grid blocks in the single lower waste panel. These values were obtained from the 10,000-year BRAGFLO calculations at specified run times. The results are screened according to these requirements. Comparisons with the BRAGFLO results from the PAVT are provided. Results of direct brine release volumes to the surface during drilling from TBM implementation of BRAGFLO_DBR are presented. Comparisons of these release volumes are also made to those from the PAVT implementation of BRAGFLO_DBR.

Three scenarios are examined. These scenarios cover the expected behavior of the repository system and their impact on direct brine release. The scenarios considered are the S1, (the undisturbed repository), the S3, (an intrusion at 1000 years into the repository that also penetrates an underlying brine pocket), and the S5, (an intrusion at 1000 years that only penetrates the repository). For direct brine release the analysis of S1 results examines the release of contaminated brine to the surface during the first intrusion into a previously undisturbed repository. The analysis of S3 results examines the release of contaminated brine to the surface during a second intrusion into the repository following a previous intrusion that penetrated the repository and an underlying brine pocket at 1000 years. The analysis of S5 results examines the

release of contaminated brine to the surface during a second intrusion into the repository following a previous intrusion that penetrated only the repository at 1000 years.

A summary of the number of vectors in Scenarios 1, 2 and 5 that satisfy the minimum requirements for direct brine release during intrusion drilling for both the TBM and PAVT implementations is shown in Table 1.

Table 1: Number of vectors that satisfy the minimum requirement for DBR releases: a comparison of TBM and PAVT

Scenario	Intrusion times (years)	Number of vectors for TBM	Number of Vectors for PAVT
S1	1,000	8	14
	5,000	13	27
	10,000	14	31
S3	1,200	59	70
	5,000	15	31
	10,000	19	25
S5	1,200	9	15
	5,000	4	12
	10,000	6	11

Figures 9 to 11 show average brine saturations in the intruded waste panel (single panel) as a function of time for Scenarios 1, 3 and 5 respectively. The plot for S1 (Figure 9) shows that mean brine saturations for TBI are very similar to the PAVT. In contrast TBM saturations are very low. This is mainly due to the use of Option D panel closure as also corroborated by Figure 12. Figure 12 shows net brine flow into waste panel (single panel) for the three scenarios. The brine flow for S1 is relatively low.

Figure 10 shows average brine saturations in the waste panel for S3. In this case the TBM saturations are comparable to those of PAVT and TBI, although slightly lower. Up to the intrusion time of 1000 years S3 saturation follows the same trend as that of S1. At the time of intrusion the average saturations sharply increase for PAVT, TBI and TBM, and remain high. Figure 12 also shows a sharp increase of net cumulative brine flow into the waste panel, and higher overall brine flows into the waste panel compared to S1 and S5. This is because Scenario 3 models an intrusion into the high-pressure brine pocket. Figures 13 and 14 show average cumulative brine flows to the repository from the intruded borehole and from anhydrite layers, respectively. As shown in Figure 13 flow from the brine pocket (from borehole at bottom of lower DRZ) is much more significant than from other units. The flows from the three anhydrite layers for S3 (Figure 14) are similar to those of S5 (Figure 16).

Figure 11 shows average brine saturations in the waste panel for S5. Here the saturations for TBM are greater than those in S1, although they are lower than S3. At the time of intrusion of 1000 years the average saturations did not sharply increase as they did in S3. This is because there is no brine pocket in this scenario. The intrusion borehole does not extend to a brine pocket. After the intrusion time of 1000 years PAVT, TBI and TBM all show an increasing saturation trend. This is because as the pressure in the repository decreases due to the intrusion, brine flows from neighboring units as shown in Figure 12. Figures 15 and 16 show the amount of brine flows into the repository from the borehole and anhydrite layers, respectively. Figure 15 shows that there is no brine flow from the borehole at the bottom of the DRZ, indicating the absence of the brine pocket. Figure 15 and 16 also indicate that the downward flow of brine through an intrusion borehole entering a waste disposal panel is small compared to the contribution that comes from the anhydrite interbeds.

Figure 17 shows scatter plots for cumulative brine volume removed to the surface during drilling as a function of volume-averaged down dip intruded waste panel brine saturation and pressure at times of intrusion for intrusion times of 5000 and 10,000 years, for Scenarios 1, 3 and 5. The plots show similar trends as those of the 1996 CCA (Helton et al., 1998, Figure 10.1.2, page 10-3). In Figure 17 the non-zero brine removed values are mainly due to S3. The saturation plots show a familiar trend where volume removed is highest for saturations between 0.6 and 0.7, with lower brine removed at lower and higher saturations. Low saturations mean lower amount of brine in the waste panel and hence lower releases. At higher residual brine saturations the amount of brine available for flow is even lower. For very high brine saturations the corresponding pressures are low because there has been less gas generation. Also, according to the response surface for bottom-hole pressure at high brine saturations bottomhole pressure is high. Both of these effects cause the brine removed to be low (Equation 1).

The volume removed vs. pressure plots show that higher brine removed is associated with intermediate pressures, consistent with Helton et al. (1998, Page 10-1) and not associated with high pressures. This is because high pressures are a result of significant gas generation and are consequently associated with a large degree of brine consumption during corrosion. Thus the occurrences of high pressure are also coincident with occurrence of low brine saturation often below residual brine saturation making flow of this brine impossible. The occurrence of high brine saturation is often accompanied by pressure below the 8MPa needed to result in flow of this brine to the surface through the borehole.

The major differences between the PAVT and TBM are: a new TBM grid, implementation of Option D panel closure, changing the molecular weight of cellulosics, and the correction to include the factor of 2π in the calculation of the productivity index and the resulting changes made to the flowing bottom-hole pressure response surfaces. The Technical Baseline Intermediate (TBI) study has shown that grid differences between the PAVT and TBM have not caused pressure and saturation differences in the repository (Hansen et al., 2002). The TBI results indicated that the grid refinements only have very minor effects on the BRAGFLO results.

Hadgu and Stein (2002) show that the effect of the molecular weight change of cellulosics is very small. Hansen et al. (2002) also showed that the effect of using a larger molecular weight of cellulosics in the TBM calculations has a marginal effect. As described in Hadgu et al. (1999), the effect of the 2π addition is to increase brine release by about a factor of 2 in the high release

cases and by a higher magnitude at the lower release cases. But as shown above TBM brine releases are low. The low brine releases during S1 and S5 for the TBM are then presumably due to the implementation of the tight Option D panel closure. Thus, the Option D panel closures are by far the most significant change for the TBM.

Use of the tight Option D panel closure isolates the intruded panel from the rest of the repository depriving DBR contributions from other panels. Unlike Scenarios 1 and 5, Scenario 3 has more significant brine releases. At intrusion time of 1200 years most of the TBM releases are greater than those of PAVT, although many of these releases are still low. Figure 13 shows that the Scenario 3 brine releases are due to large amounts of brine flowing from the high pressure brine pocket to the intruded panel as a result of the borehole intrusion. The higher S3 releases in the TBM implementation, when compared to S1 and S5 releases, are also directly attributed to the effectiveness of the Option D panel closure system in isolating the intruded panel from the rest of the repository. Because the intruded panel during an S3 scenario is isolated from the rest of the repository, most of the brine that flows up through the borehole from the underlying brine pocket is confined to the panel that was intruded. In the PAVT implementation this brine, which entered the intruded panel, could readily flow across the panel closure or around it through the disturbed rock zone. Thus in the PAVT brine from the underlying brine pocket was more easily distributed across the entire repository resulting in smaller volumes of brine and less brine saturation in the intruded panel in the PAVT compared to the TBM.

Table 2: Comparison of brine release predictions of TBM and PAVT calculations for Scenario S3

Output Variable Description	Intrusion Time (yrs)	TBM Implementation (R1)					PAVT Implementation (R1)				
		10th	50th	Mean	90th	Max.	10th	50th	Mean	90th	Max.
Brine Volume (m^3)	1,200	0.0	0.2	6.9	21.2	42.0	0.0	2.5	5.5	14.6	75.8
	5,000	0.0	0.0	1.5	1.7	45.6	0.0	0.0	3.7	12.4	63.7
	10,000	0.0	0.0	1.4	1.4	37.3	0.0	0.0	4.0	8.1	99.7

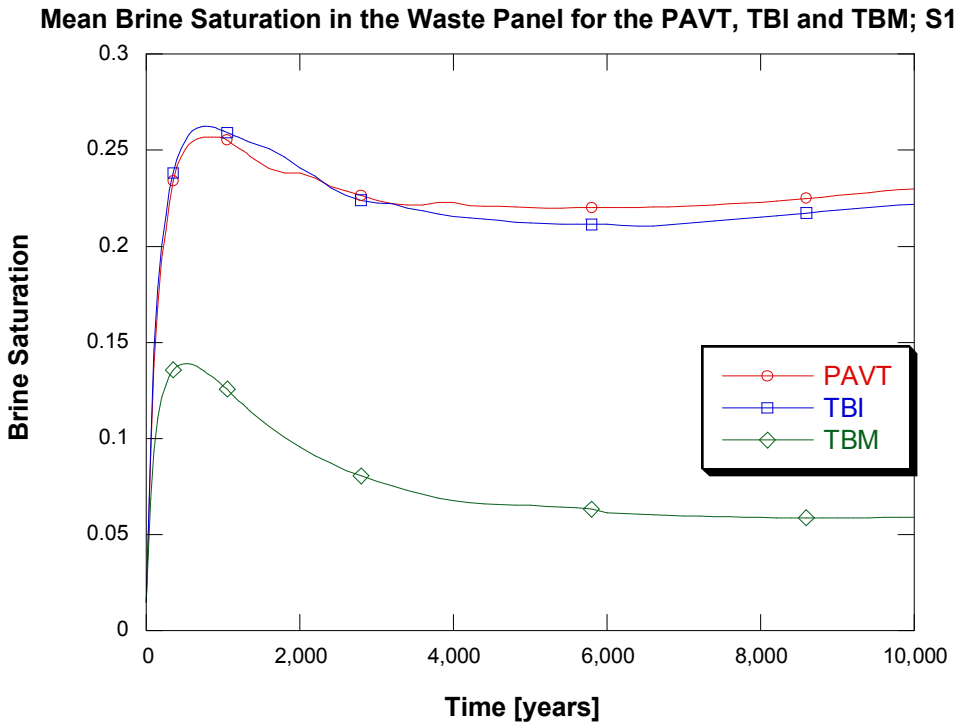

Figure 9: Mean Volume Averaged Brine Saturation in the Waste Panel for the PAVT,TBI, and TBM; S1

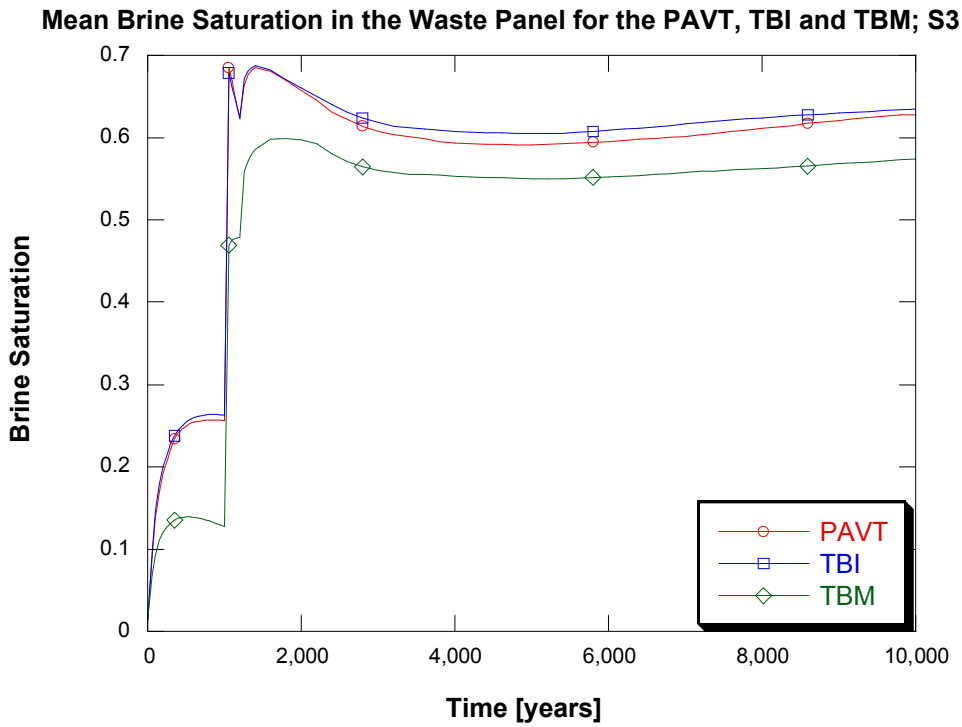

Figure10: Mean Volume Averaged Brine Saturation in the Waste Panel for the PAVT, TBI and TBM, S3

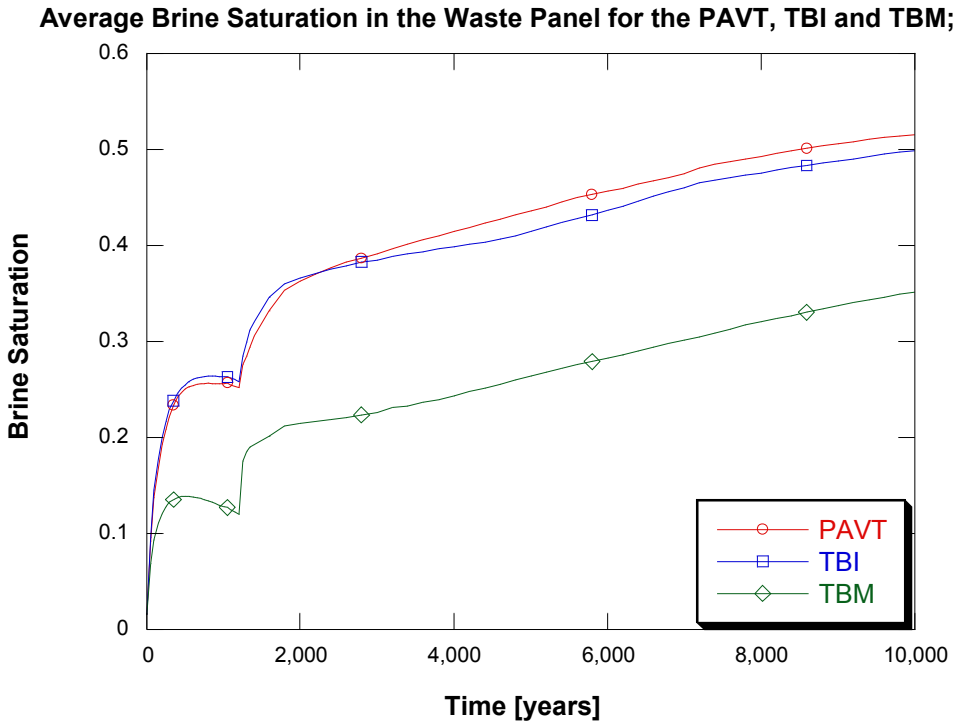

Figure11: Mean Volume Averaged Brine Saturation in the Waste Panel for the PAVT, TBI and TBM; S5

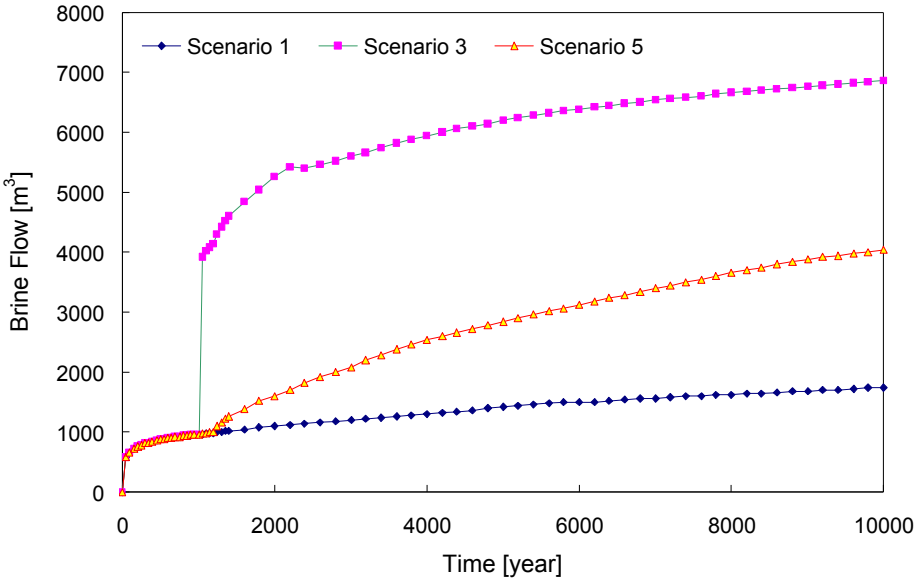

Figure12: Net brine flow into intruded waste panel: TBM

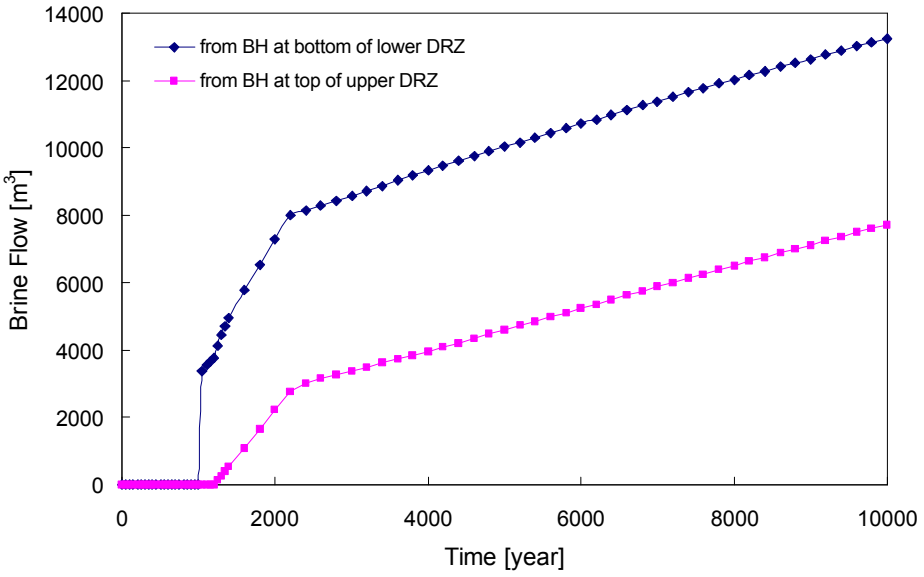

Figure13: Cumulative brine flow from borehole to repository (lower single panel) for Scenario 3: TBM

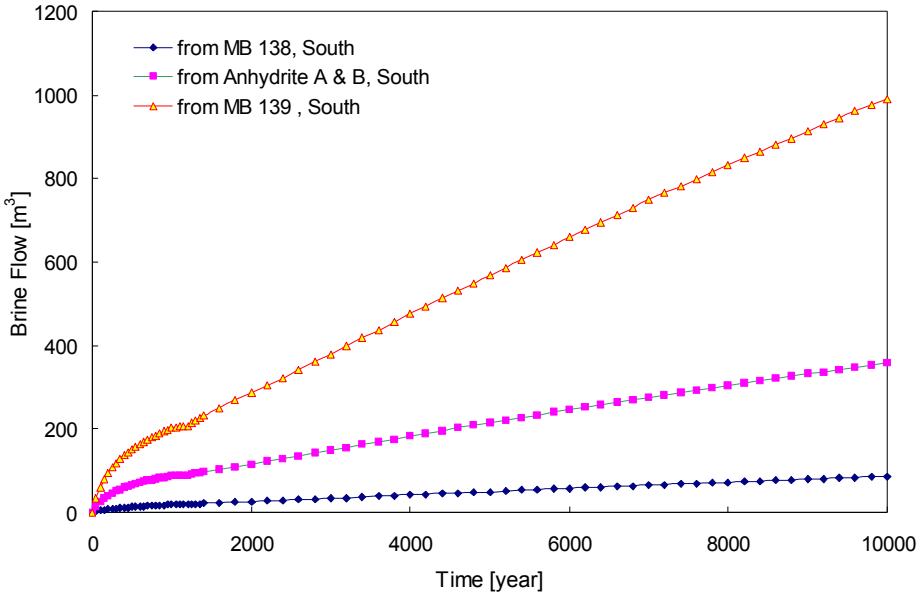

Figure14: Cumulative brine flow from anhydrite layers to repository (lower single panel) for Scenario 3: TBM

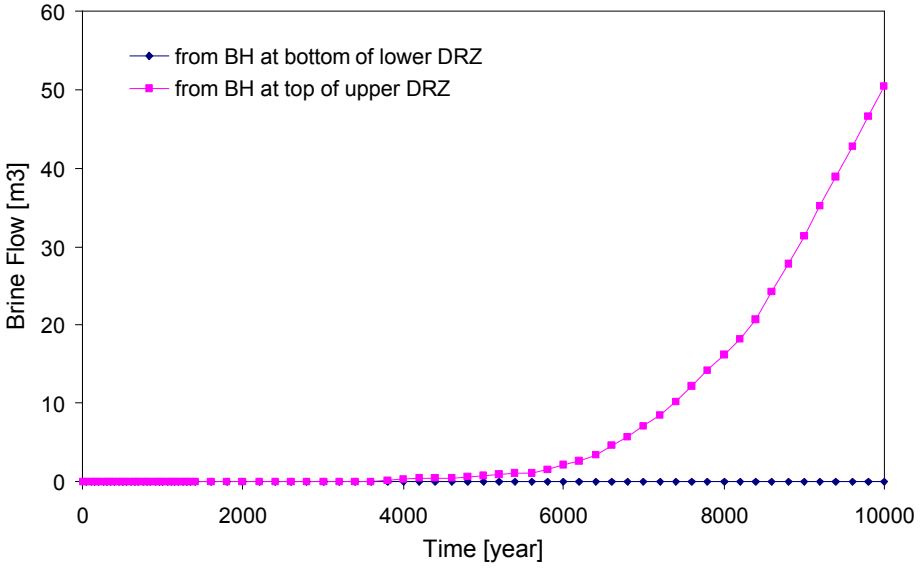

Figure15: Cumulative brine flow from borehole to repository (lower single panel) for Scenario 5: TBM

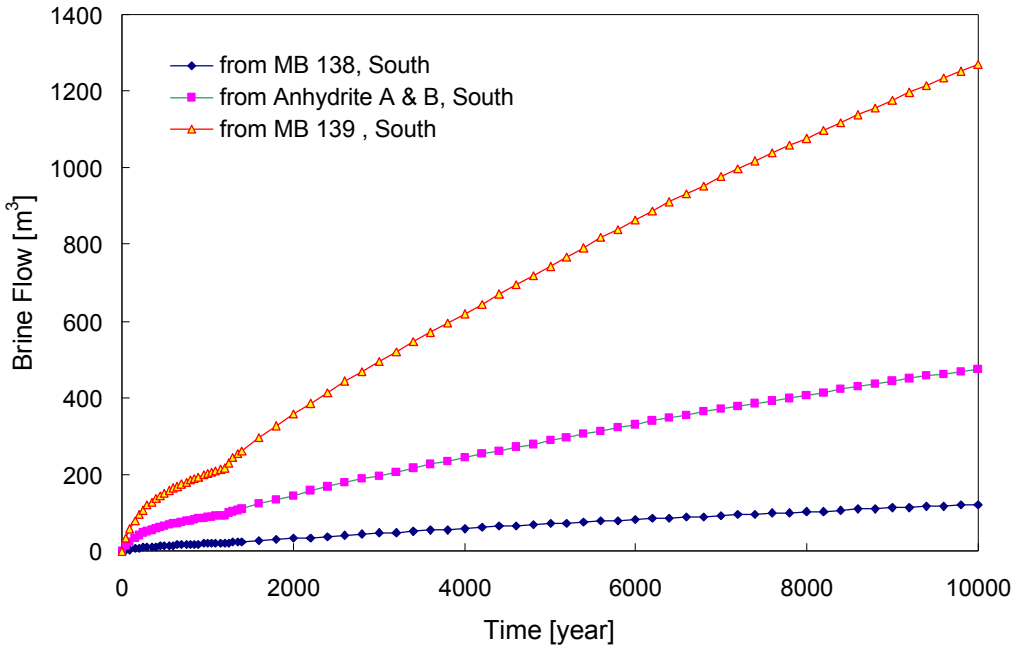

Figure16: Cumulative brine flow from anhydrite layers to repository (lower single panel) for Scenario 5: TBM

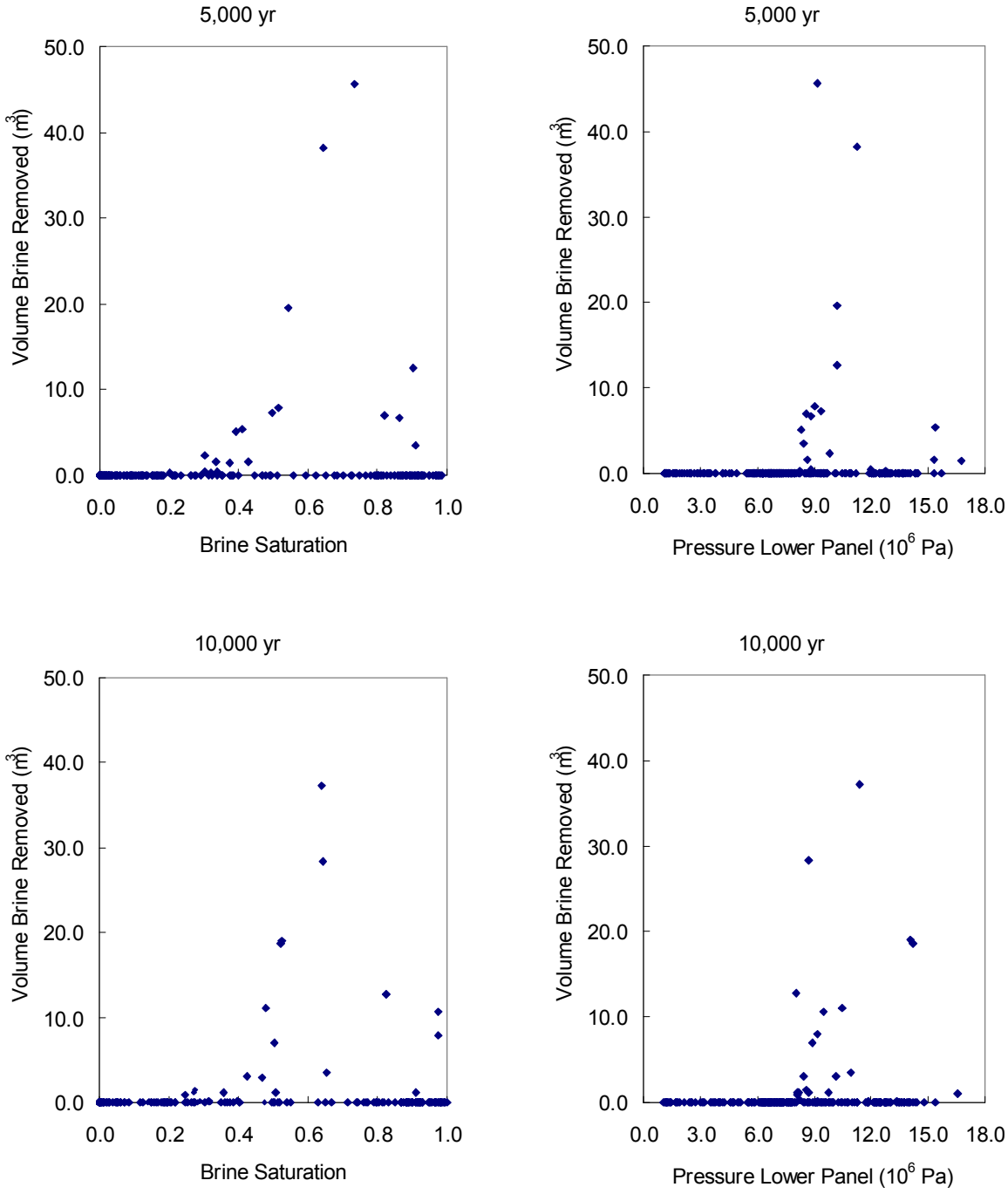

Figure17: Scatterplots for volume of brine removed from repository due to direct brine release from a down-dip waste panel for scenarios 1, 3, 5 versus volume averaged brine saturation and pressure in that panel

4. CONCLUSION

This report documents an analysis of DBR for the TBM analysis. The major changes introduced in the TBM over the previous baseline were: a new TBM grid, implementation of Option D panel closure, changing the molecular weight of cellulosics, and a correction to include the factor of 2π in the calculation of the productivity index and the resulting changes made to the flowing bottom-hole pressure response surfaces. Results show that for the TBM, Scenarios 1 and 5 result in low direct brine release. The releases during these scenarios from the TBM implementation are less than the corresponding releases from the PAVT implementation. The TBI study showed that the TBM grid changes have very little effect on results. The cellulosics molecular weight change and the 2π correction in the productivity index equation also have marginal effect on results. Thus, the main reason for the low brine releases for Scenarios 1 and 5 is the implementation of Option D panel closure. Use of the tight Option D panel closure isolates the intruded panel from the rest of the repository, depriving DBR contributions from other panels. Unlike Scenarios 1 and 5, Scenario 3 has more significant brine releases. At intrusion time of 1200 years many TBM releases are greater than those of PAVT, although many of these releases are still low. Plots show that the Scenario 3 brine releases are due to large amounts of brine flowing from the high pressure brine pocket to the intruded panel as a result of the borehole intrusion. The higher S3 releases, compared to S1 and S5, are also directly attributed to the effectiveness of the Option D panel closure system in isolating the intruded panel from the rest of the repository

5. ACKNOWLEDGMENT

The authors would like to acknowledge the valuable contributions to this work provided by Christi D. Leigh (SNL), Mario J. Chaves (SNL) and David S. Kessel (SNL). This research is funded by WIPP programs administered by the Office of Environmental Management (EM) of the U.S. Department of Energy. Sandia is a multi program laboratory operated by Sandia Corporation, a Lockheed Martin Company, for the United States Department of Energy's National Nuclear Security Administration under Contract DE-AC04-94AL85000.

6. REFERENCES

Hadgu, T. and Stein, J. S. (2002), Addendum for Regression Test of BRAGFLO 4.10.01. ERMS# 520778, Sandia WIPP Records Center, Sandia National Laboratories, Carlsbad, NM.

Hadgu, T., Vaughn, P., Bean, J., Johnson, D., Johnson, J., Aragon, K., Helton, J., Modifications to the 96 CCA direct brine release calculations, Memo to Mel Marrieta dated Nov. 2, 1999. ERMS# 511627, Sandia National Laboratories, Albuquerque, NM., 1999.

Hansen, C., C. Leigh, D. Lord, and J. S. Stein, (2002), BRAGFLO results for the technical baseline migration; ERMS# 523209, Sandia WIPP Records Center, Sandia National Laboratories, Carlsbad, NM.

Helton, J. C., J. E. Bean, J. W. Berglund, F. J. Davis, K. Economy, J. W. Garner, J. D. Johnson, R. J. MacKinnon, J. Miller, D. G. O'Brien, J. L. Ramsey, J. D. Schreiber, A. Shinta, L. N. Smith, D. M. Stoelzel, C. Stockman, and P. Vaughn, (1998),Uncertainty and sensitivity analysis results

obtained in the 1996 performance assessment for the Waste Isolation Pilot Plant; SAND98-0365, Sandia National Laboratories, Albuquerque, NM.

Hurtado, L. D., M. K. Knowles, V. A. Kelley, T. L. Jones, J. B. Ogintz, and T. W. Pfeifle, (1997), WIPP shaft seal system parameters recommended to support compliance calculations, SAND97-1287, Sandia National Laboratories, Albuquerque, NM.

MacKinnon, R. J., G. Freeze, and H-N. Jow, (1997), Supplemental summary of EPA-mandated performance assessment verification test (all replicates) and comparison with the compliance certification application calculations, ERMS# 246702, Sandia WIPP Records Center, Sandia National Laboratories, Albuquerque, NM.

Poettmann, F. H. and P. G. Carpenter, (1952), Multiphase flow of gas, oil, and water through vertical flow strings with application to the design of gas-lift installations, *Drill Prod Pract,* American Petroleum Institute, pp. 257-317.

MacKinnon, R. J., Summary of uncertainty and sensitivity analysis results for the EPA-mandated performance assessment verification test, ERMS# 246912, Sandia WIPP Records Center, Sandia National Laboratories, Albuquerque, NM.

Thompson, T. W., and F. D. Hansen, (1996), Long-term performance of panel closures, memorandum to M. G. Marietta, August 2, 1996; ERMS# 240418, Sandia National Laboratories, Albuquerque, NM.

U.S. DOE (U.S. Department of Energy), (1996), Title 40 CFR Part 191 Compliance certification application for the Waste Isolation Pilot Plant, DOE/CAO-1996-2184, U.S. Department of Energy, Waste Isolation Pilot Plant, Carlsbad Area Office, Carlsbad, NM.

EPA (U.S. Environmental Protection Agency), (1998), 40 CFR Part 194: Criteria for the certification and re-certification of the Waste Isolation Pilot Plant's compliance with the disposal regulations: certification decision; final rule. Federal Register, Vol. 63, p. 27396, Office of Radiation and Indoor Air, Washington, D.C..

Vaughn, P., (1996), FEP Screening Analysis, S1: Verification of 2D-radial flaring using 3D geometry, pp. 13-15, ERMS# 415853, Sandia WIPP Records Center, Sandia National Laboratories, Albuquerque, NM.